

Wide Band Microstrip Patch Antenna with Enhanced Gain using FSS Structure

Tapas Tewary¹ , Smarajit Maity² , Avisankar Roy³ , Sunandan Bhunia⁴ 

¹Assistant Professor, Academy of Technology, Hooghly, West Bengal, tapas.tewary@aot.edu.in

²Assistant Professor, Academy of Technology, Hooghly, West Bengal, smarajit.maity@aot.edu.in

³Associate Professor, Haldia Institute of Technology, Haldia, West Bengal, avisankar.roy@gmail.com

⁴Associate Professor, Central Institute of Technology, Kokrajhar, Assam, s.bhunias@cit.ac.in

Abstract— This paper suggests a slotted ground ‘S’-shaped low profile planar microstrip patch antenna for wideband and high gain operation. The suggested antenna has physical dimensions of 20mm × 14mm × 1.6mm having a fractional bandwidth of 111% having the operating impedance bandwidth 22.55GHz (9.12 GHz to 31.67 GHz). At 19 GHz, maximum gain of 3.9 dBi is attained. An equivalent circuit model corresponding to suggested antenna is designed by ADS software and assessed with the simulated and measured antenna results. Frequency Selective Surface (FSS) of single layer has been placed at optimum position at a distance of 15 mm below the antenna for further improvement of the overall gain of the suggested antenna. Combination of suggested antenna and 6 × 6 FSS configuration increases peak gain to 9.4 dBi maintaining the same antenna bandwidth. The FSS unit cell of dimension 6.5mm × 6.5mm × 1.6mm is used. Design of the antenna is done using commercially available electromagnetic simulator (CST Microwave Studio), and the simulated results are verified by suitable antenna measurement technique using standard microwave test bench. Given FSS integrated antenna has an overall physical volume of 39mm × 39mm × 15mm which makes it ideally suited for high-gain long-range applications.

Index Terms—FSS (Frequency Selective Surface), High gain, Equivalent Circuit, Wideband

I. INTRODUCTION

Wireless communication is essential in today's world. Without wireless connection, life would be challenging given how reliant we are on the internet, data transmission, etc. Antennas are necessary for wireless communication systems to function successfully at both the transmitter and receiver. Among many types of antennas, microstrip patch antennas are relatively inexpensive to design and develop due to their simple two-dimensional physical geometry. Due to these attractive features, the microstrip patch antenna (MPA) has been used extensively in different applications and intensive research work is going on over the past three decades for modifying the antenna structures. Microstrip patch antennas provide more benefits and more promising futures than traditional antennas. They are easier to fabricate and conform to low volume, light weight, inexpensive, smaller in size etc. Moreover, microstrip patch antennas are capable of frequency agility, beam scanning with omnidirectional

patterning, multiple polarization, broad bandwidth, multi frequency operation and feed line flexibility etc. But narrow impedance bandwidth is a major problem of this type of antenna to meet the ever increasing demand of modern communication system for wireless operation as well as for satellite and radar application. Another major drawback is low gain. Due to these, research on patch antenna is mainly focused on designing a patch antenna with high gain having a wide operating bandwidth. Various approaches were investigated for achieving multiband, wideband operation of patch antennas with multiple resonant frequencies in multiple wireless applications. Also, modern communication industry is demanding 5G compatible antenna in mid frequency band (starting from 24.25 GHz) due to heavy usage in low frequency band. Comprehensive review of 5G antennas in different band and performance enhancement techniques are discussed in [1]. Also, broadband antenna has been achieved by transposed 'S' shape patch having defective ground plane [2], utilizing monopole antenna topology [3] and flower shaped slot loaded patch [4]. Ultra wideband characteristics are obtained using multi slotted patch [5], hexagonal shaped patch [6]. Rectangular microstrip patch antenna with slot loaded finite ground plane is proposed for compact broadband operation [7]. Antenna gain has been significantly enhanced by utilizing numerous substrate layers having rectangular slotted patch [8], by revising 'S' shape patch [9], by utilizing H- shape ground plane and SIW (substrate integrated waveguide) patch [10], by reforming parameters of antenna [11-12]. High -10 dB operating bandwidth has been attained by increasing height of the patch in a non-uniform manner [13]. A multiband antenna is presented in [14] using an extra slotted conical shaped patch integrated with a triangular patch. Antenna gain has been significantly enhanced by utilizing EBG (Electronic Band Gap) arrangements in the ground plane [15], by utilizing arrays of antenna in radiating patch [16], by using the concept of mode superposition [17], by developing array of reflector [18], using combination of two different kinds of radiating elements [19]. Combination of Frequency Selective Surface (FSS) and antenna is successfully used to enhance antenna gain and is reported in recent research [20-25].

This article introduces a microstrip line fed 'S' shape wide band microstrip patch antenna which is obtained by modifying the reference structure's ground plane and radiating patch by adding slots of proper dimension in proper location. The electrical dimension of the antenna is $0.6\lambda \times 0.4\lambda \times 0.05\lambda$ where λ indicates operating wavelength corresponds to 9.12 GHz. A large impedance bandwidth 22.55 GHz (9.12 GHz-31.67GHz) is achieved by proposed antenna which covers part of X band (8 GHz to 12 GHz) followed by Ku band (12 GHz to 18 GHz), K band (18 GHz to 27 GHz) and LMDS (Local Multipoint Distribution Service) band (26 GHz to 31.3 GHz). Also it covers a part of Ka band (26.5 GHz to 40 GHz) and some portion of 5G application band (24.25 GHz to 52.6 GHz). At 19 GHz maximum gain of 3.9 dBi is attained. Further to enhance antenna gain a single-layered 6×6 FSS having the dimension of $39 \times 39 \text{ mm}^2$ is positioned beneath the proposed antenna at a suitable gap of 15 mm. Peak gain of 9.4 dBi is achieved for FSS combined antenna. Maximum gain enhancement of 6 dB is observed for FSS combined antenna in comparison with antenna without FSS. The proposed antenna

and FSS combined antenna are suitable for short range and long range wireless communication respectively.

This manuscript is organized as follows: Antenna architecture is discussed in Section II. Evolution of the proposed antenna is discussed in Section III. Variations of -10 dB impedance bandwidth depending on different antenna parameters are discussed in Section IV. Experimental results with regard to reflection coefficient, gain, efficiency, radiation pattern and simulated surface current distribution are described in Section V. Section VI presents equivalent circuit model of the proposed antenna. Section VII discussed the model of FSS combined antenna structure for gain enhancement and corresponding simulated and measured results are discussed in detail. Concluding remarks are presented in section VIII.

II. ANTENNA ARCHITECTURE

Fig. 1(a) and Fig. 1(b) show radiating patch and ground plane architecture of the proposed antenna respectively. The ‘S’ shaped patch is constructed by loading two same dimension rectangular shape slots at optimum position. Ground plane structure is modified by loading with identical four rectangular slots in such a way that wide band characteristics can be achieved through better impedance matching.

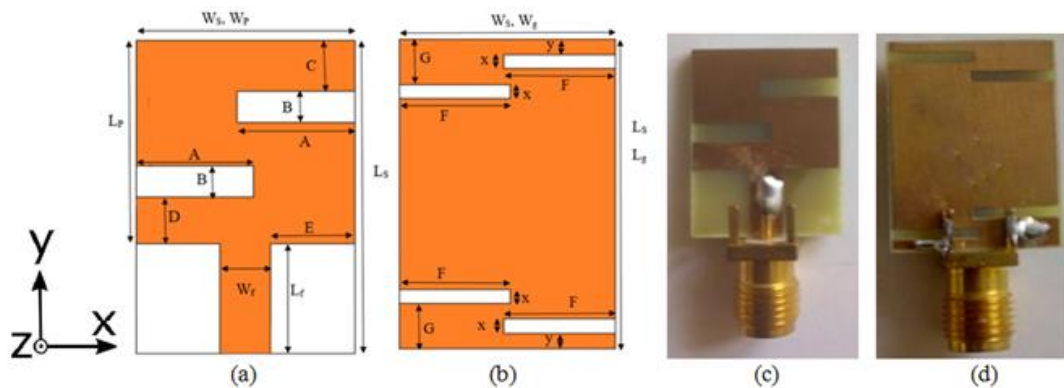


Fig. 1.(a)Antenna patch and (b) Ground plane (c) Fabricated Patch and (d) Fabricated Ground

TABLE I. PROPOSED ANTENNA AND UNIT CELL FSS PARAMETERS AND THEIR VALUE IN MM

Parameter Name	Optimal value in mm	Parameter Name	Optimal value in mm	Parameter Name	Optimal value in mm
L_s, L_g	20	B	2	L_{FSS}, W_{FSS}	6.5
W_s, W_g	14	C	3.25	I	2.35
h(antenna)	1.6	D	3	J	0.7
L_p	13	E	5.4	K	0.8
W_p	14	F	7.2	L	1.4
L_f	7	G	2.9	M	6.1
W_f	3.2	X	0.9	g	0.2
A	7.5	y	1	h(FSS)	1.6

The comprehensive figures of antenna patch and ground plane structures are shown in Fig. 1(a) and Fig. 1(b). Fabricated antenna’s patch and ground is shown in Fig. 1(c) and Fig. 1(d). Values of all parameters of the presented antenna are tabulated in Table I.

III. EVOLUTION OF PRESENTED ANTENNA

Fig. 2 illustrates step by step (step 1 - step 7) design of presented antenna. All the simulation results related to evolution of the antenna is done using commercially available electromagnetic simulator (CST Microwave Studio).

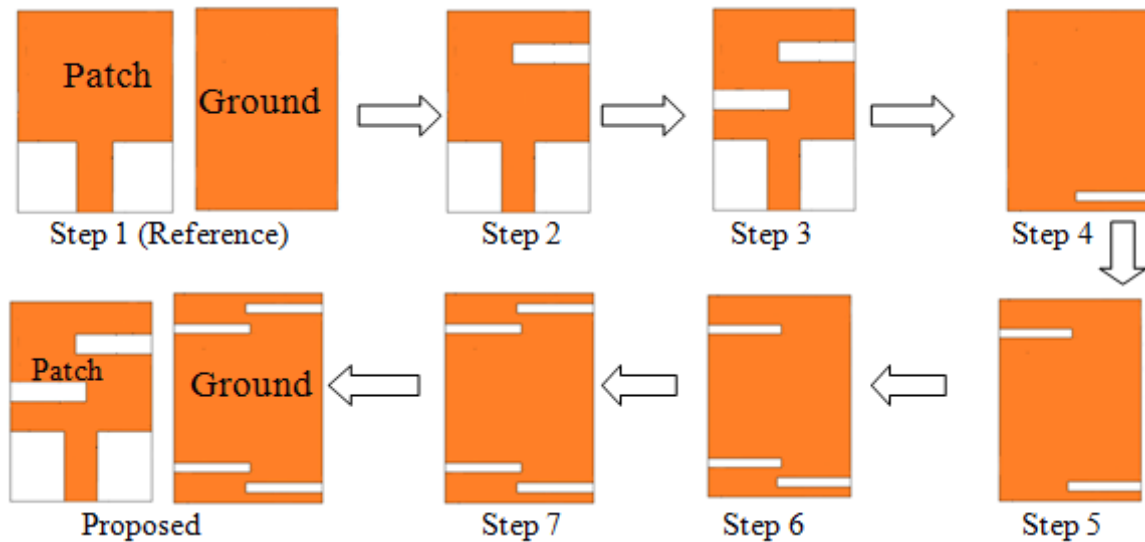


Fig.2.Designed steps of proposed antenna

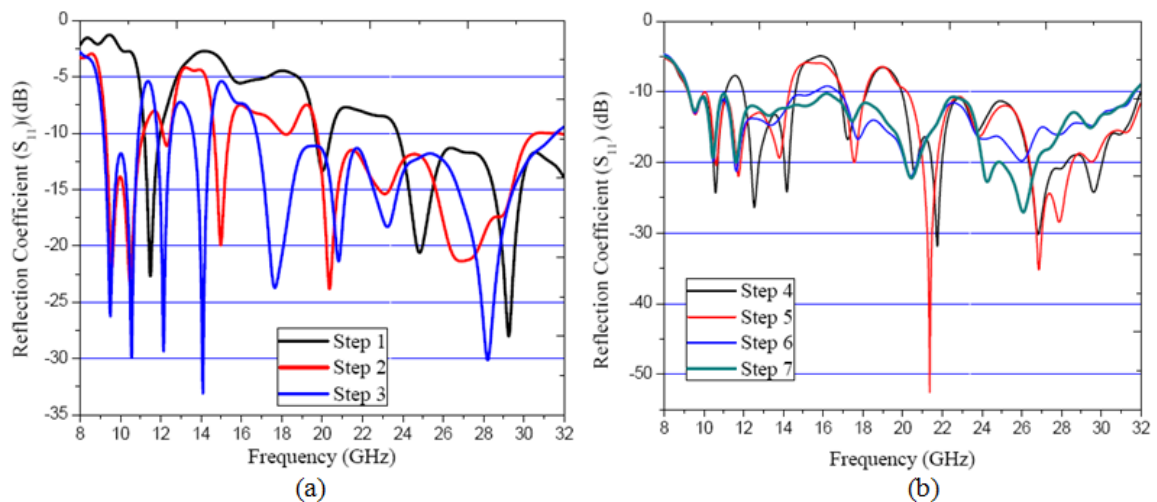


Fig. 3. (a)Variation of S_{11} for step 1, step 2 and step 3 (b) Variation of S_{11} for step 4 up to step 7

Fig. 3(a) and Fig. 3(b) show reflection coefficients of all seven design steps. Step 1 illustrates reference antenna having rectangular patch for radiating and finite ground plane. But impedance matching is not so good for this finite ground plane. So, reference antenna poorly resonates at 20 GHz. Then two rectangular slots are loaded in patch to create multiple frequency bands as shown in step 2 and step 3. From reflection coefficient corresponding to step 3 it is seen that there are 7 frequency bands starting from 9 GHz to 31 GHz. Antenna's input impedance is still not around the impedance of the SMA connector (i.e 50 Ω) for the entire band of interest and due to poor impedance

matching wide band characteristic is not achieved. To obtain impedance matching within a large frequency band, ground plane is modified by loading four rectangular shaped slots of optimum length and width at proper location in symmetry. In step 4 ground plane is modified by loading a rectangular slot in bottom left corner of the ground plane. Due to better impedance matching some frequency bands merge and only four frequency bands are now present. Similarly in step 5, same dimension slot is loaded in the ground plane at top left corner and thus only 3 frequency bands are present now. In step 6 again identical slot is loaded in the ground plane at bottom left corner and in this step only 2 frequency bands are achieved. Finally in step 7 similar dimension slot is loaded in ground plane at top right corner in symmetry. It can be observed that due to slot introduction in ground plane close multiple frequency bands merged together and wide band characteristics is achieved due to the effect of stagger tune phenomenon [27].

IV. PARAMETRIC STUDIES

Through rigorous parametric studies optimal values of all the parameters are finalized. On the patch there are two identical slots in symmetry with the dimension of $A \times B$. Fig. 4 and fig. 5 illustrates reflection coefficients for the variation of the value of A when parameter B is kept constant. It can be observed that for optimal value of $A = 7.5$ mm and $B = 2$ mm the desired broadband characteristics are obtained.

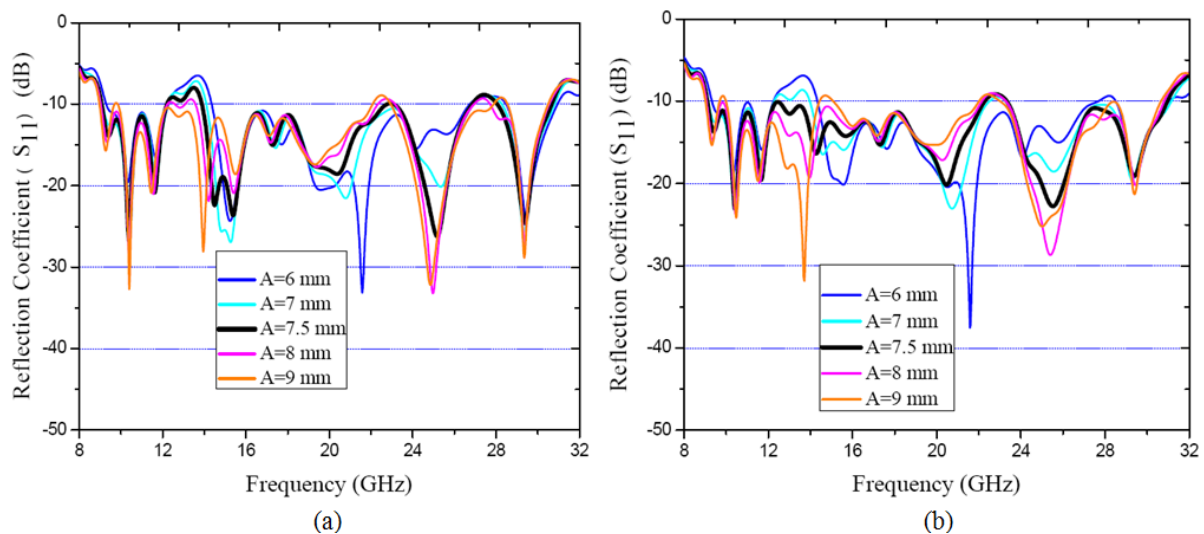


Fig.4. (a) S_{11} for variation of A when $B = 1$ mm (b) S_{11} for variation of A when $B = 1.5$ mm

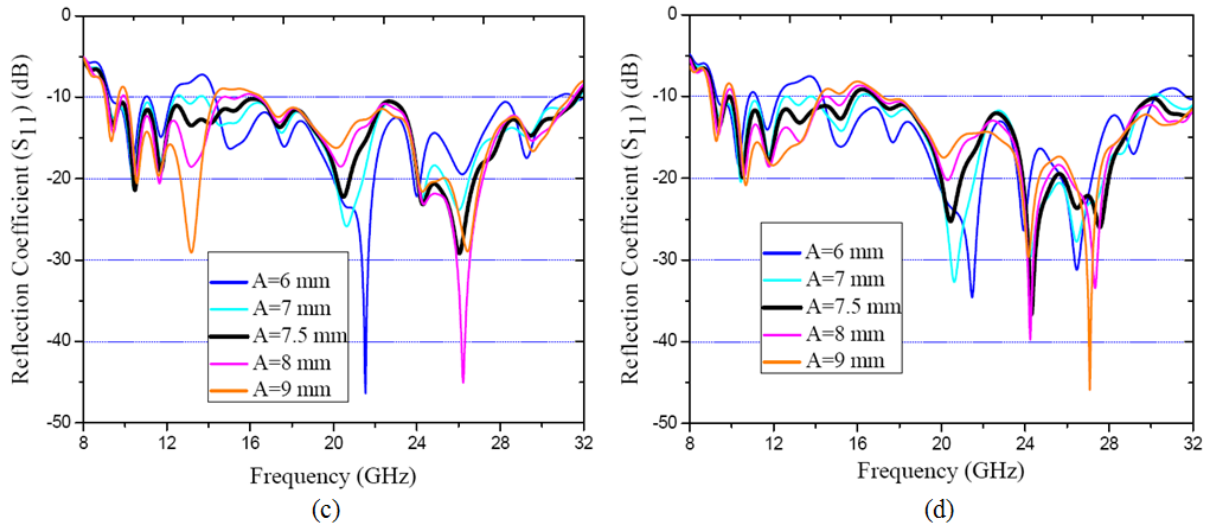


Fig. 5.(c) S_{11} for variation of A when B=2 mm (d) S_{11} for variation of A when B=2.5 mm

Again optimal positions of the slots on the radiating patch are determined by the parameter ‘C’ and ‘D’. Fig. 6 shows the corresponding reflection coefficient variation. For ‘C’=3.25 mm and ‘D’=3 mm broadband characteristics is obtained.

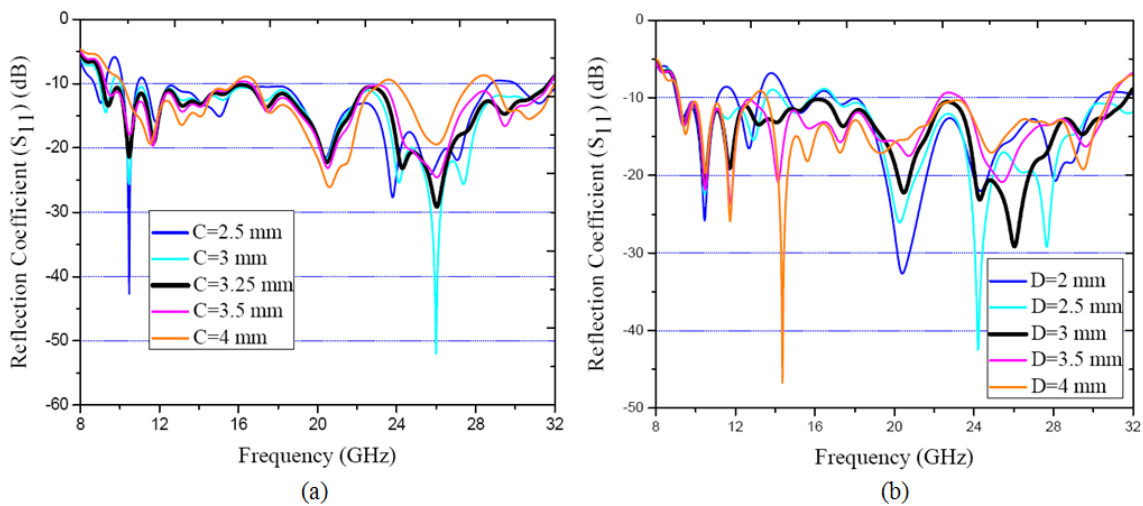


Fig. 6. (a) S_{11} with variation of parameter C (b) S_{11} with variation of parameter D

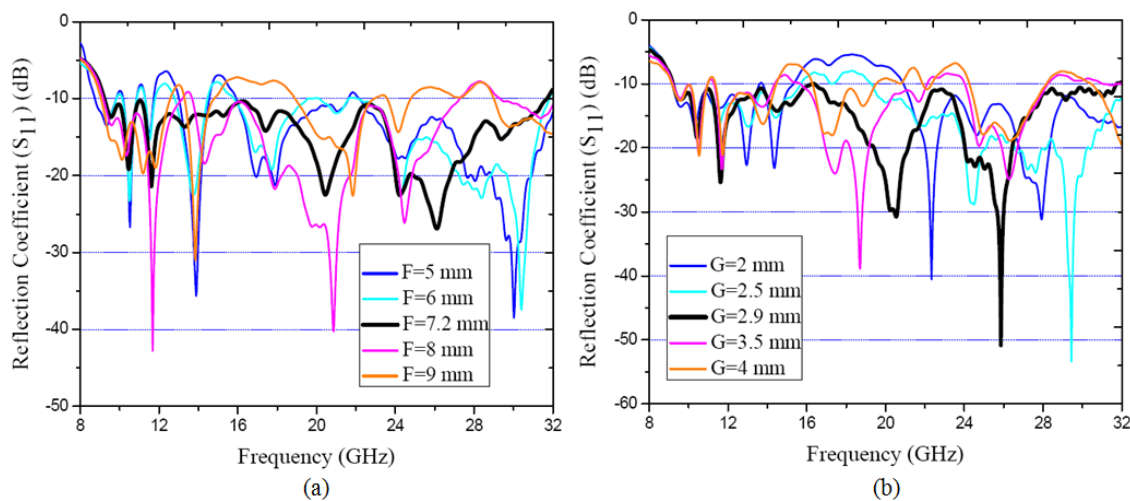


Fig. 7. (a) S_{11} for variation of parameter F (b) S_{11} for variation of parameter G



On the ground plane there are four slots in perfect symmetry. Slots in the ground plane help to achieve better impedance matching. Fig. 7 and Fig. 8 illustrate reflection coefficient variation for the variation of the parameter (F, G, x and y) value.

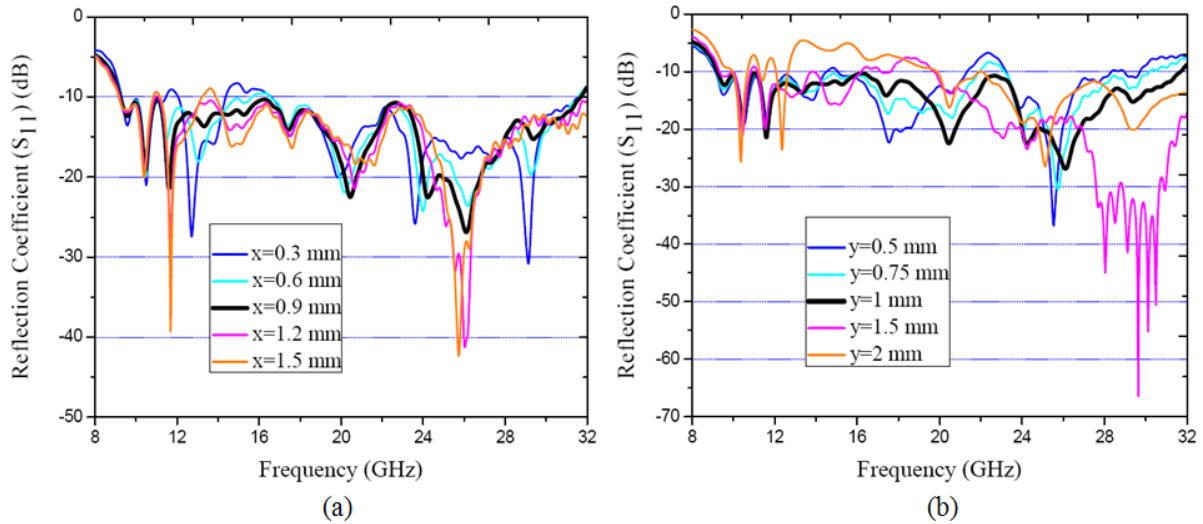


Fig. 8. (a) S_{11} with variation of parameter x (b) S_{11} with variation of parameter y

V. SIMULATED AND MEASURED RESULT

The suggested antenna is developed by FR-4 substrate and measured using standard microwave test bench. Fig. 9(a) and Fig. 9(b) shows measured and simulated result for reflection coefficients (S_{11}) and efficiency proposed antenna respectively. The proposed antenna achieves strong resonance property at 10.46 GHz, 11.62 GHz, 20.44 GHz, 24.26 GHz and 26.1 GHz. Fig. 9(b) shows simulated efficiency range from 57% to 36% and measured efficiency range from 58% to 37%. Fig. 10(a) and Fig. 10(b) illustrate peak gain (dBi) of proposed antenna and gain measurement set up. At 19 GHz, 3.9 dBi peak gain was achieved experimentally.

From measured gain and measured radiation pattern efficiency is calculated by using the following equation.

$$Directivity \approx \frac{41253}{\theta_{1d} \times \theta_{2d}} \text{ and Gain} = Efficiency \times Directivity \quad [26]$$

Where θ_{1d} = Half-power beamwidth in one plane (in degree) (E plane) and

θ_{2d} = Half-power beamwidth in a plane at a right angle to the other (in degree) (H plane)

As efficiency is calculated from measured parameters, this can be considered as equivalent to measured efficiency.

Fractional Bandwidth of the proposed antenna is found to be 111% with the following formulae.

$$\text{Fractional bandwidth} = \left(\frac{F_H - F_L}{F_C} \times 100 \right) \% = 111 \% ; F_H = 31.67 \text{ GHz} ; F_L = 9.12 \text{ GHz} ; F_C = 20.395 \text{ GHz}$$

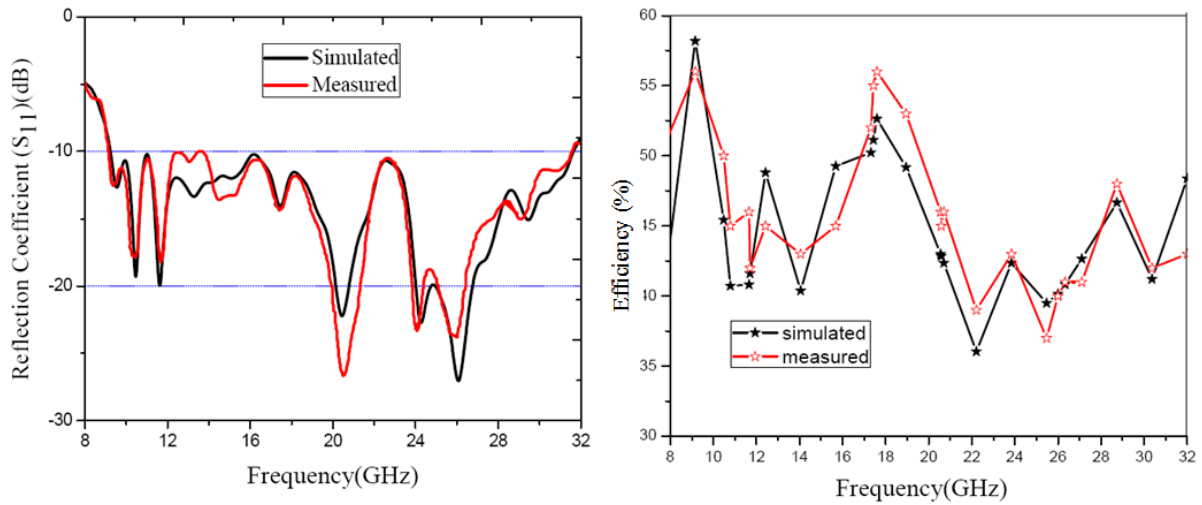


Fig. 9. (a) Simulated and measured Reflection coefficient (b) Simulated and measured efficiency

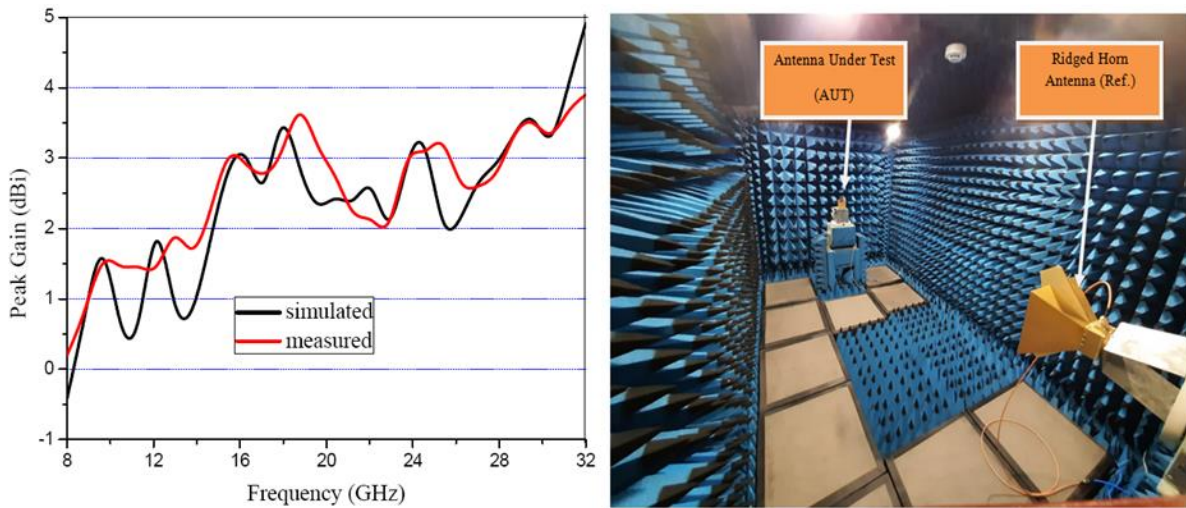


Fig. 10. (a) Simulated and measured Peak Gain (b) Gain measurement setup (Grateful to: CIT, Kokrajhar, Assam, India)

Fig. 11 displays the surface current distribution for the frequencies of 10.46 GHz, 11.62 GHz, 20.44 GHz, and 26.1 GHz. According to conventional current distribution pattern, fundamental mode is excited for lowest resonant frequency and higher order modes along with the harmonics of the fundamental mode are excited at succeeding high resonant frequencies. Wideband has been achieved due to the combined effect of different resonating modes.

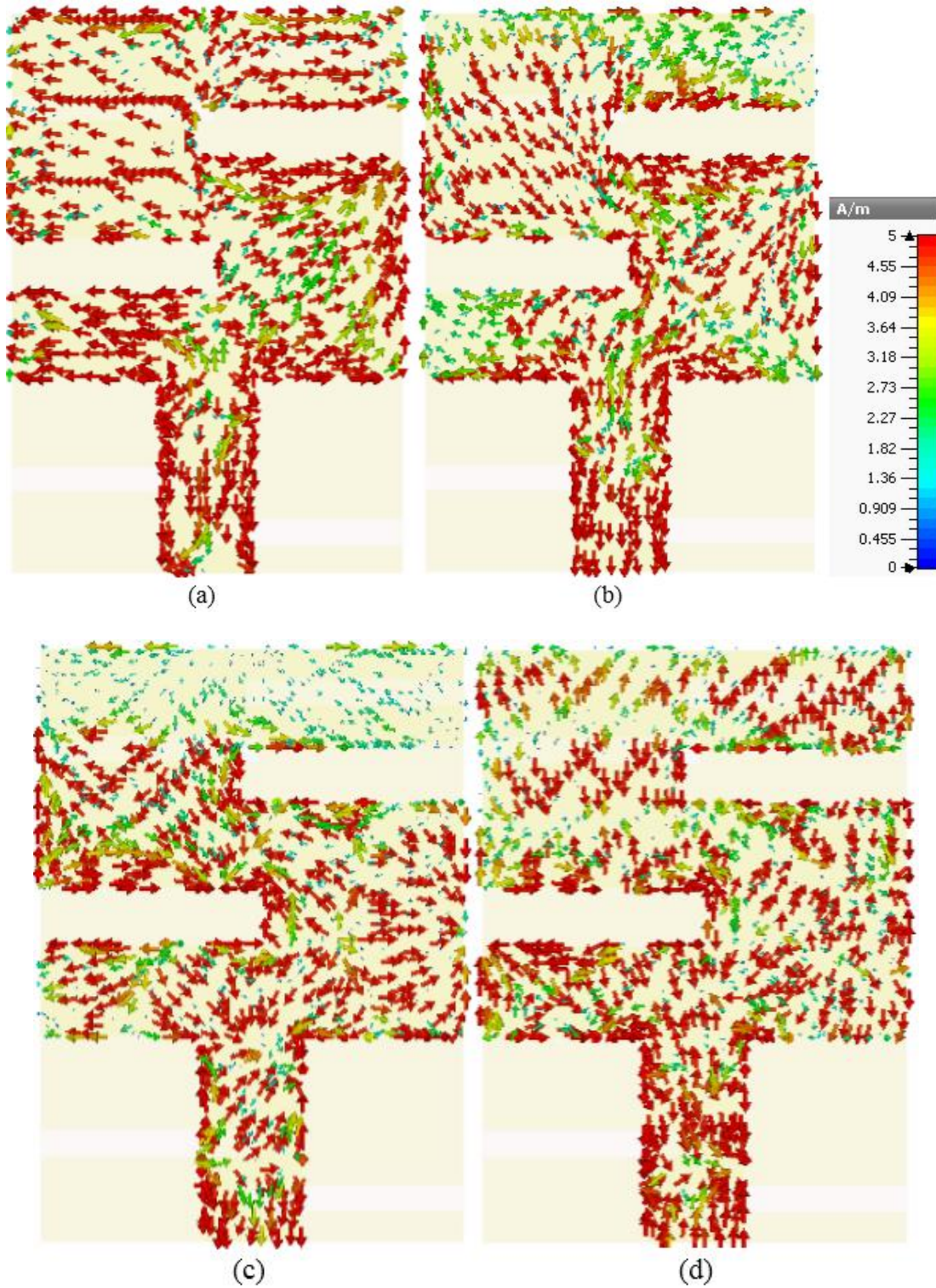


Fig. 11. Distribution of surface current at (a) 10.46 GHz (b) 11.62 GHz (c) 20.44 GHz (d) 26.1 GHz

The computed and measured normalized E plane co-pol and cross-pol radiation patterns at 10.46 GHz, 11.62 GHz, 20.44 GHz and 26.1 GHz are shown in Fig. 12(a)-(d). Also, it can be shown that the results of the simulation and the measurements are fairly similar. At low frequency it shows only two

main lobes. As frequency increases multiple prominent lobes can be observed. Fig. 13(a)-(d) illustrates H plane simulated and measured co-pol and cross-pol radiation patterns at four resonant frequencies (10.46 GHz, 11.62 GHz, 20.44 GHz and 26.1 GHz). Due to the stimulation of higher order modes, radiation patterns at high frequencies are more distorted than at low frequencies.

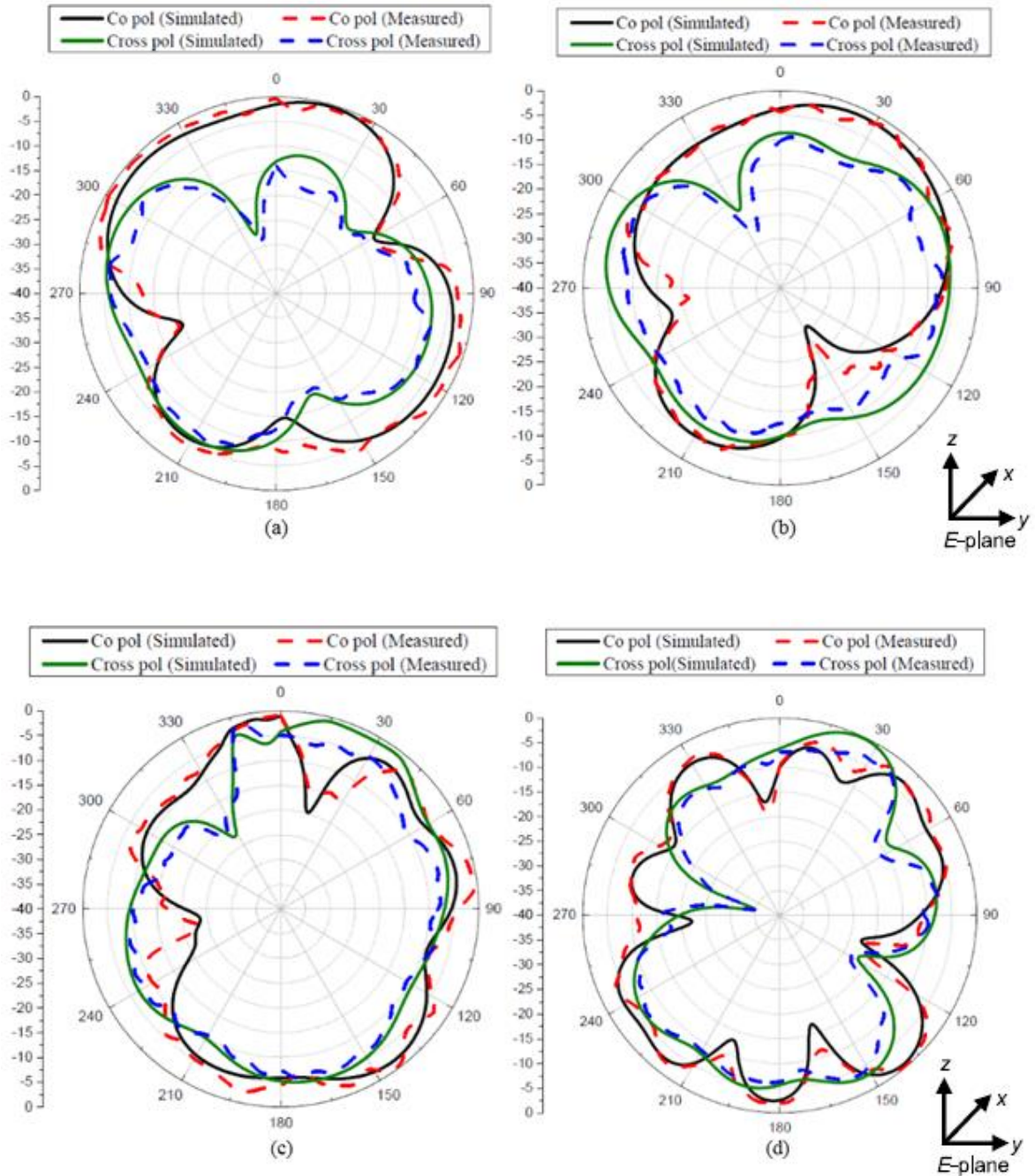


Fig. 12. Normalized E field co-pol and cross pol at (a) 10.46 GHz (b) 11.62 GHz (c) 20.44 GHz (d) 26.1 GHz

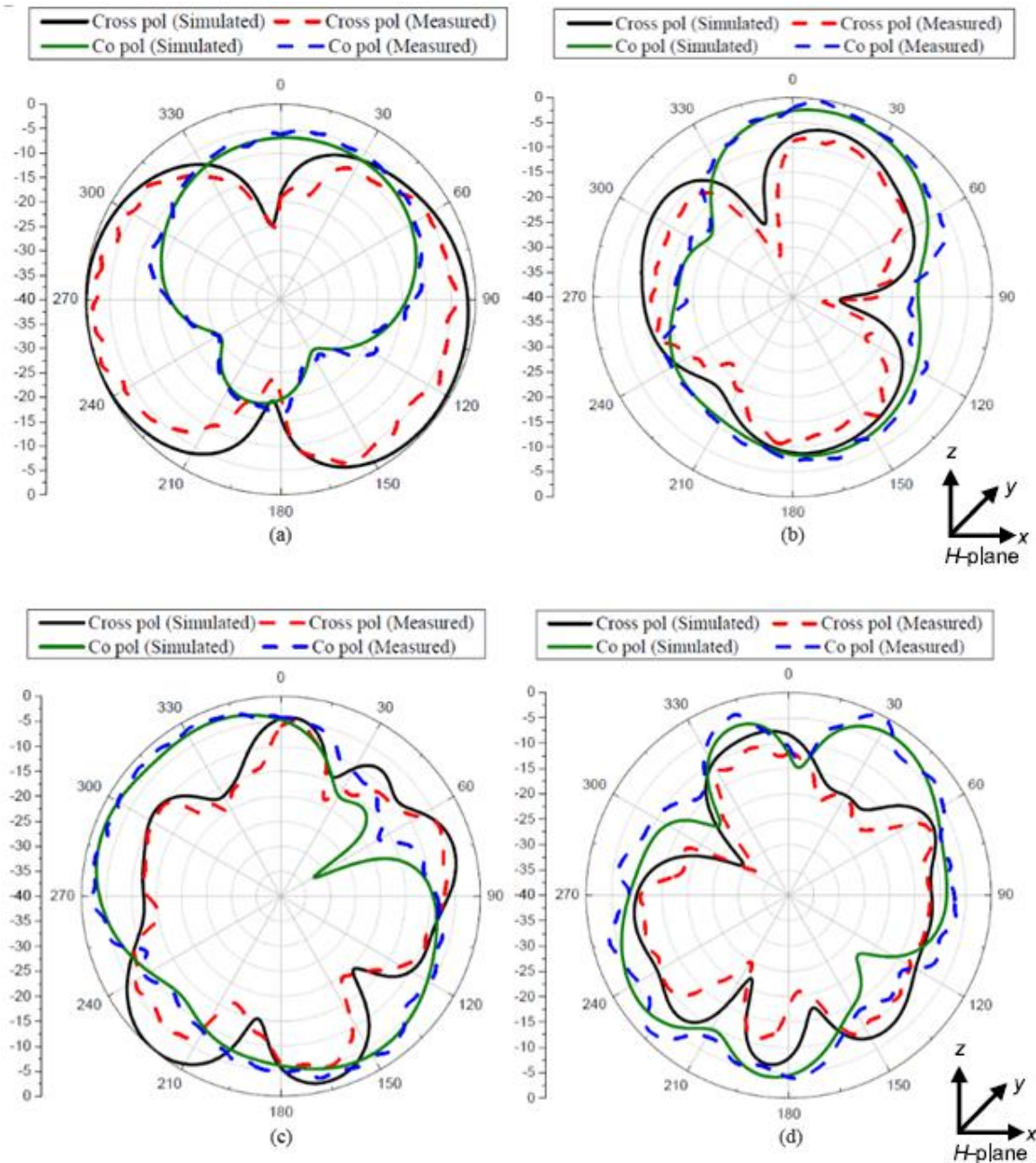


Fig. 13. H field co-pol and cross pol at (a) 10.46 GHz (b) 11.62 GHz(c) 20.44 GHz (d) 26.1 GHz

VI. EQUIVALENT CIRCUIT ANALYSIS

Fig. 14 shows equivalent RLC model circuit of the presented antenna which consists of six sections of RLC circuit connected in parallel corresponding to six resonant frequencies. Fig. 15 compares measured reflection coefficient (S_{11}) with the frequency response of the equivalent lumped circuit model of the antenna analyzed by ADS software and the simulation results using CST software. R-L-C values of each section corresponding to each resonant frequency are calculated by the following formulas (1-3). All resonant frequencies (f) and corresponding values of inductor (L), resistor (R) capacitor(C), 3 dB BW (GHz) and quality factor (Q) are tabulated in table II.

$$f = \frac{1}{2\pi\sqrt{LC}} \dots (1); Q = 2\pi fCR \dots (2) \text{ and } Q = \frac{f}{(BW)_{3dB}} \dots (3)$$

TABLE II. Q, R, L, C VALUES OF THE EQUIVALENT R-L-C CIRCUIT MODEL

Freq(GHz)	3 dB BW(GHz)	Q	R(Ω)	L(pH)	C (pF)
10.46	0.25	41.84	61.8	22.474	10.301
11.62	0.32	36.3	43.6	16.451	11.403
17.45	1.8	9.7	35.7	33.568	2.4782
20.44	0.8	25.6	55.95	17.018	3.5627
24.26	0.9	27	43.1	10.472	4.1098
26.1	1.3	20.1	53	16.079	2.3126

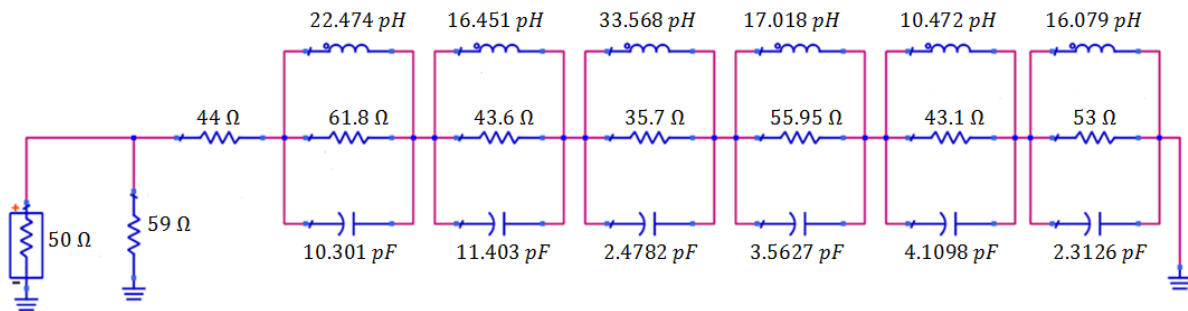


Fig. 14. Equivalent RLC circuit model of the proposed antenna

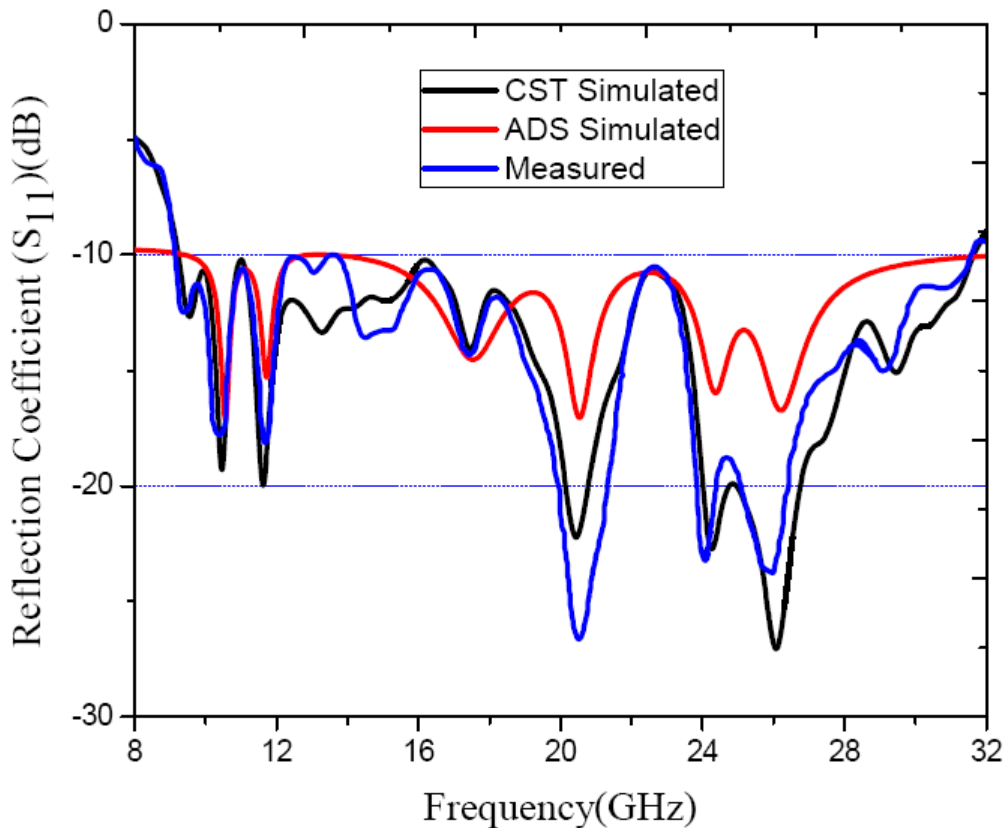


Fig. 15. Comparison of Simulated S_{11} of the antenna by ADS, CST MWS with measured S_{11} of the antenna



VII. DESIGN OF FSS EMBEDDED ANTENNA

To increase antenna gain without compromising the impedance bandwidth, the antenna has been integrated with single layer band reject FSS structure which stops the band frequency 9 GHz to 31 GHz. Depending on the design criteria, level of attenuation, band stop or band pass frequency, appropriate FSS elements are chosen. FSS elements are categorized into four basic types. In this work type 3 FSS structure which is solid interior (may be square, hexagon, Circle etc.) or plate types are chosen. Then slots are loaded to obtain required reflection characteristics [20], [23], [27]. Proposed FSS unit cell displayed in Fig. 16 (a) and FSS unit cell parameters are given in the TABLE I. Three identical circles shaped slots with diameter ‘L’ with same separation (‘K’) are loaded on square shaped patch. Though FSS structure is infinite ideally but to achieve the design goal, 6×6 FSS ($39\text{mm} \times 39\text{mm}$) structure is taken. The fabricated model of the 6×6 FSS and the FSS combined antenna structure are shown in Fig. 16(b). Fig. 16(c) shows reflection coefficient of FSS combined antenna for different distance between antenna and FSS.

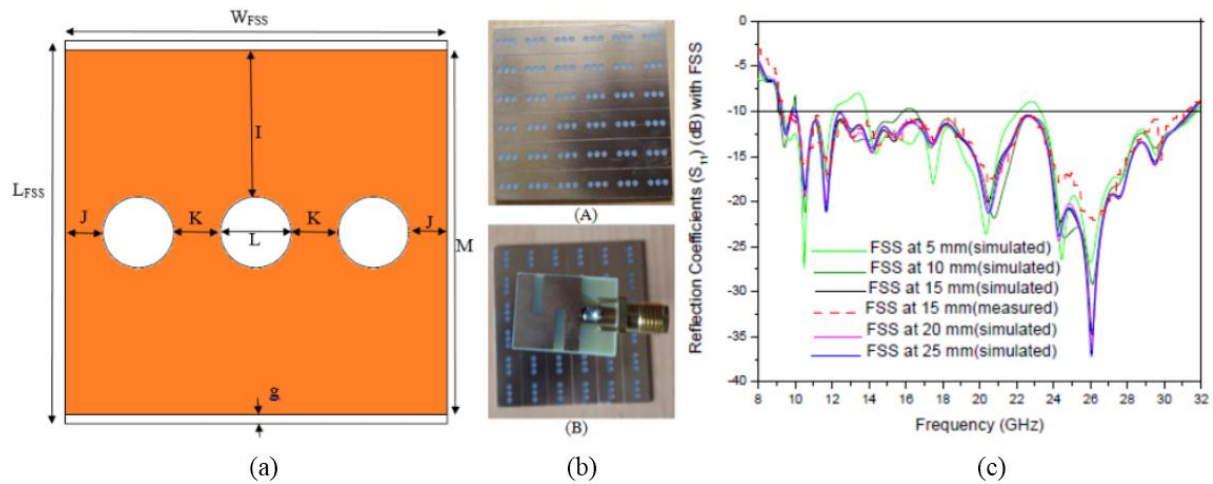


Fig.16. (a) FSS unit cell (b) Fabricated proto type (A) 6×6 FSS and (B) combined structure (c) S_{11} of FSS integrated antenna

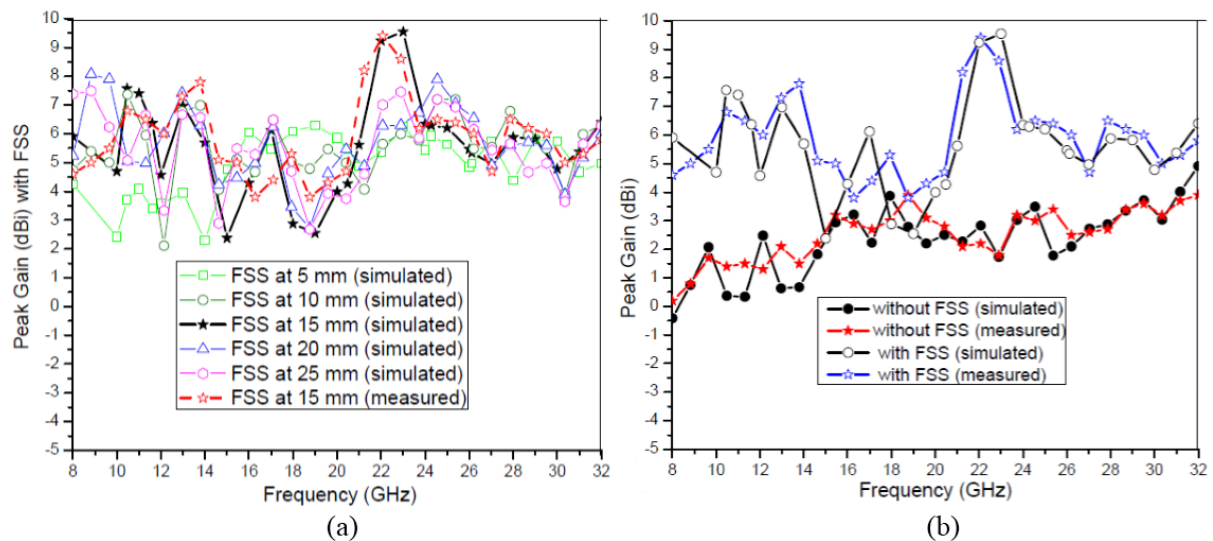


Fig.17. (a) FSS integrated antenna peak gain (b) Gain increment at 15 mm gap between antenna and FSS



For minimum 15 mm air gap distance between antenna and FSS broadband characteristic same as only antenna is observed. The measured and simulated reflection coefficients of proposed FSS combined antenna are displayed in Fig. 17(a). Similarly Fig. 17(b) displays maximum gain of the FSS combined antenna for the same air gap distance. For 15 mm air gap maximum gain of 9.4 dBi is observed. Peak gain of the FSS combined antenna is recorded as 9.4 dBi. More than 6 dB gain increment can be achieved at 10.46 GHz, 11.62 GHz and 26.1 GHz by using FSS.

Fig. 18 and 19 show normalized simulations as well as measures of the co-pol & cross-pol patterns of radiation for the FSS coupled antenna in E (YZ) & H (XZ) plane respectively for all the resonant frequencies. It can be noticed that radiation patterns for FSS integrated antenna are highly directive and front lobe to back lobe ratio is also large. As a result high gain is achieved throughout the band of interest.

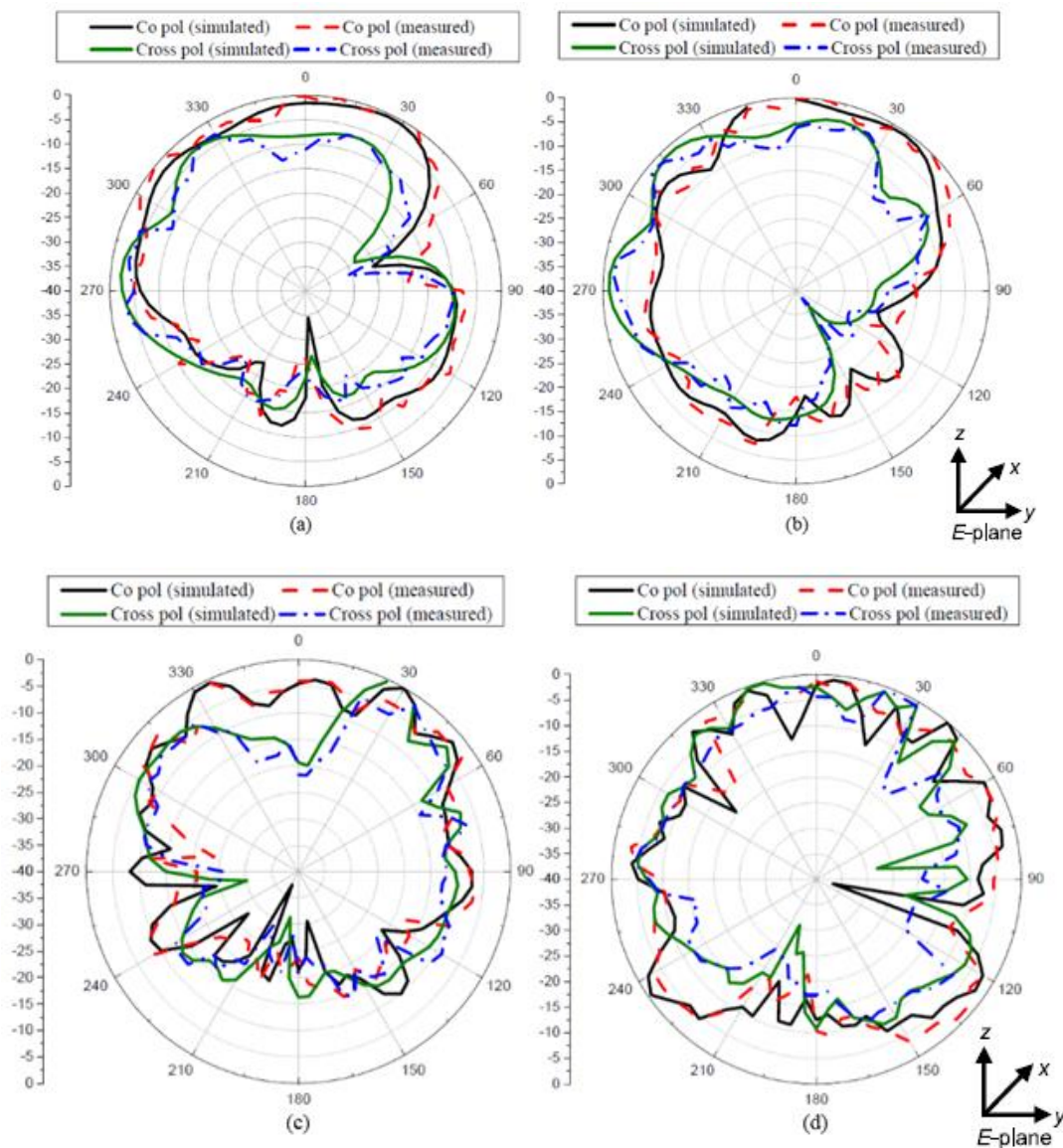


Fig. 18. E field co-pol and cross pol at (a) 10.46 GHz (b) 11.62 GHz (c) 20.44 GHz (d) 26.1 GHz with FSS

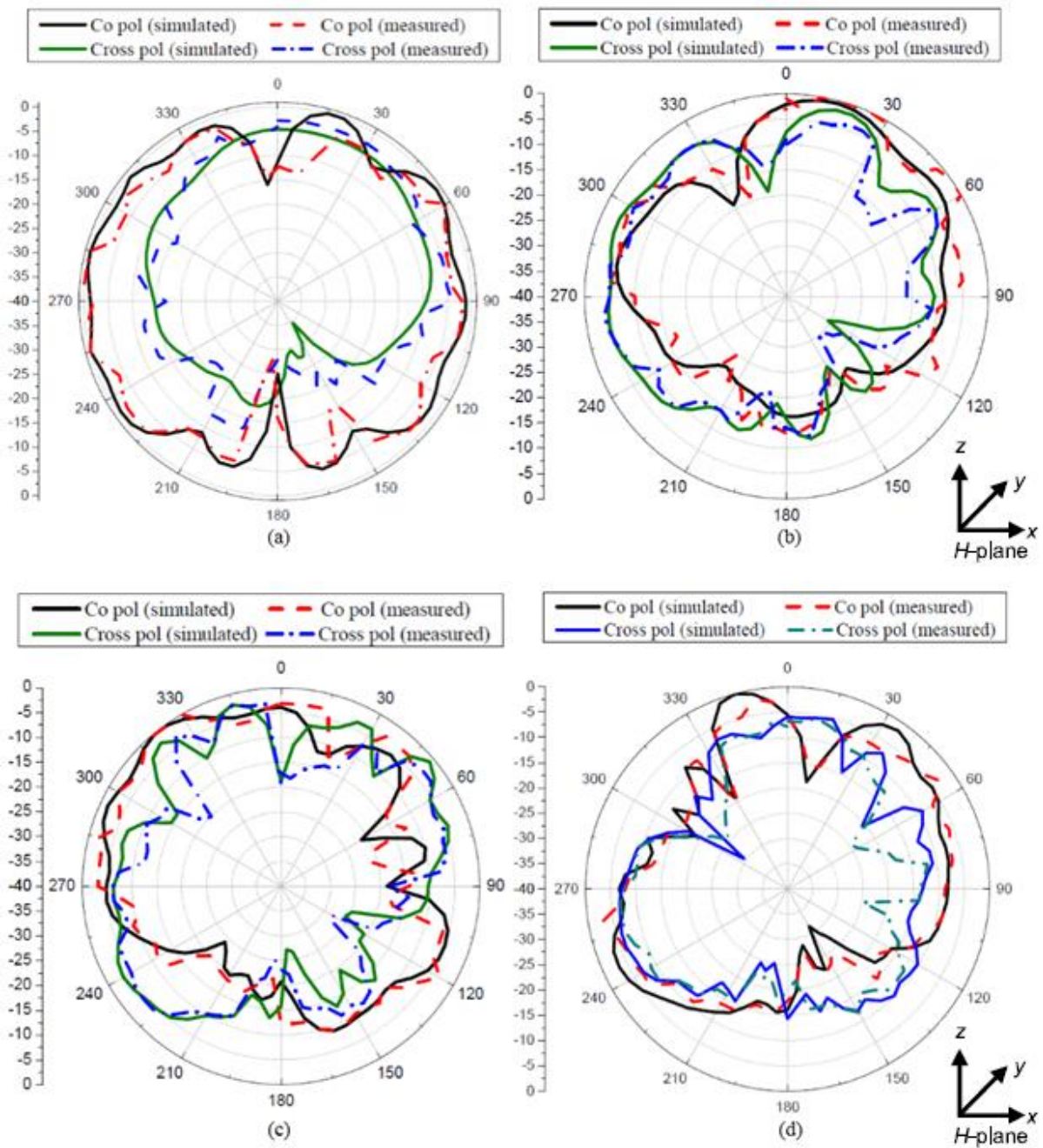


Fig. 19. H field co-pol and cross pol at (a) 10.46 GHz (b) 11.62 GHz (c) 20.44 GHz (d) 26.1 GHz with FSS

Fig. 20 illustrates simulated front lobe to back lobe ratio (FBR) both for antenna without FSS and antenna with FSS. It can be seen that for antenna without FSS, FBR (dB) varies from 2 to 18, where as for antenna using FSS, FBR (dB) varies from 7 to 24. Also it can be observed that for most of the frequencies in the desired spectrum FBR for FSS combined antenna is much higher than antenna without FSS.

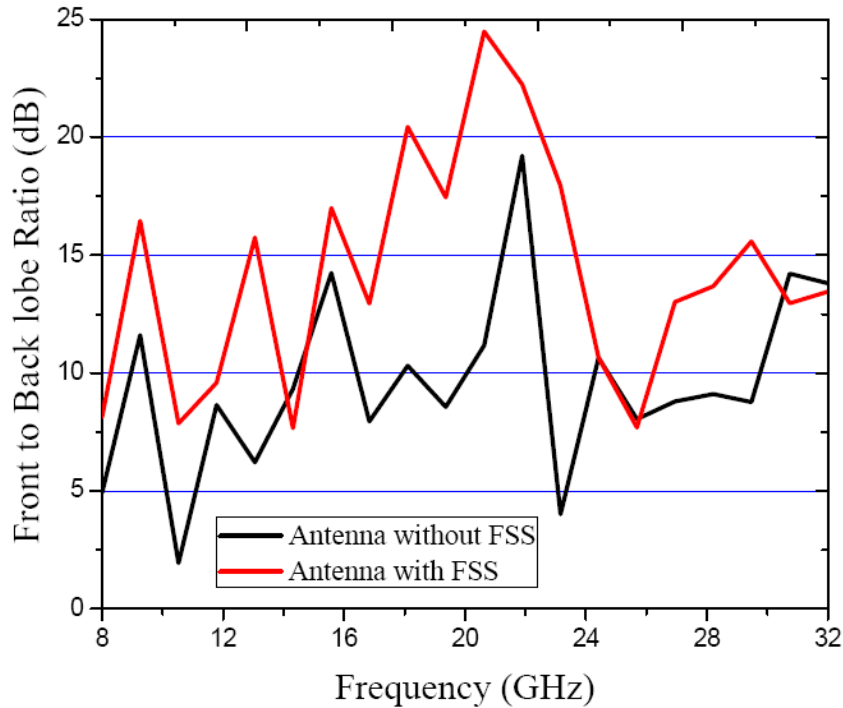


Fig. 20. Simulated Front to back lobe Ratio for only antenna and for FSS combined antenna

VIII. CONCLUSION

This article introduces line fed microstrip wideband high gain patch antenna having hybrid radiating patch with slot loaded ground plane surface. This work presents a wideband ‘S’-shaped microstrip patch antenna with slotted ground plane. The suggested antenna achieves large impedance bandwidth of 22.55 GHz (9.12 GHz-31.67 GHz) with a fractional bandwidth of 111%. Moreover, it offers a peak gain of 3.9 dBi at 19 GHz. Also, it is seen that the measured results are in good agreement with the frequency response of the equivalent lumped circuit model of the antenna (proposed) analyzed by ADS software and the simulation results using CST software. Integrating single-layer FSS with antenna increases gain and directivity even further. Maximum gain of 9.4 dBi obtained at 22.1 GHz for FSS combined antenna. For short-range communications proposed antenna without FSS structure may be used and for long-range communication applications the presented FSS integrated antenna may be used successfully. From this, we conclude that this antenna can be used in wireless communications, satellite communications, satellite services, RADAR applications, 5G communication applications etc.

REFERENCES

- [1] S. kumar, A. S. Dixit, R. R. Malekar, H. D. Raut, and L.K. Shevada, “Fifth Generation Antennas: A Comprehensive Review of Design and Performance Enhancement Techniques”, *IEEE Access*, vol. 8, pp. 163568–163593, 2020.
- [2] M. Samsuzzaman and M. T. Islam, “Inverted S-Shaped Compact Antenna for X-Band Applications”, *The Scientific World Journal*, pp.1-11, May 2014.
- [3] M. A. A. Aziz, N. Seman and T. H. Chua, “Microstrip antenna design with partial ground at frequencies above 20 GHz for 5G telecommunication systems”, *Indonesian Journal of Electrical Engineering and Computer Science*, vol. 15, no. 3, pp.1466–1473, September 2019.
- [4] I. Aggarwal, S. Pandey and M. R. Tripathy, “A High Gain Super Wideband Metamaterial Based Antenna”, *Journal of Microwaves, Optoelectronics and Electromagnetic Applications*, vol. 20, no. 2, pp. 248-273, June 2021.

- [5] N. M. Awad and M. K. Abdelaziz, "Multislot microstrip antenna for ultrawideband application", *Journal of King Saud University Engineering Science*, vol. 30, pp. 38-45, December 2018.
- [6] S. Mukherjee, A. Roy, S. Maity, T. Tewary, Dr. P. P. Sarkar and Dr. S. Bhunia, "A Design of Dual Band-Notched UWB Hexagonal Printed Microstrip Antenna", *International Journal of Microwave and Wireless Technologies*, April 2022.
- [7] S. Bhunia, A. Roy and P. P. Sarkar, "Compact wideband dual frequency (dual band) microstrip patch antenna for wireless communications", *URSI Asia-Pacific Radio Science Conference (URSI AP-RASC)*, pp. 1357-1360. 201613
- [8] A. M. Tamim, S. S. Islam, Md. A. R. Chowdhury and Md. I. Hossain, "Design of a High Gain Microstrip Patch Antenna for X-band Satellite Applications", *International Conference on Computer, Communication, Chemical, Material and Electronic Engineering (IC4ME2)*, February 2018.
- [9] A. G. Ambekar, A. A. Deshmukh, V. A. P. Chavali and K. P. Ray, "Modified S-Shape Microstrip Antennas For Dual Polarized Multiband And Wideband Response", *9th International Conference on Advances in Computing and Communication (ICACC)*, November 2019.
- [10] M. F. Nakmouche, D. E. Fawzy, A.M.M.A. Allam, H. Taher and M. F. A. Sree, "Dual Band SIW Patch Antenna Based on H-Slotted DGS for Ku Band Application", *7th International Conference on Electrical and Electronics Engineering (ICEEE)*, April 2020.
- [11] R. Abirami, E. Gnanamanoharan, S. Sivagnanam and K.P.Priya, "Design of Compact Microstrip Patch Antenna for K Band and KU Band Applications," *International Conference on System, Computation, Automation and Networking (ICSCAN)*, July 2020.
- [12] R. Przesmycki, M. Bugaj and L. Nowosielski, "Broadband Microstrip Antenna for 5G Wireless Systems Operating at 28 GHz", *Electronics*, vol. 10, no. 1, pp. 1-19, 2021.
- [13] S. Dey and N. C. Karmakar, "Design of novel super wide band antenna close to the fundamental dimension limit theory", *Scientific Reports, nature research*, 2020.
- [14] Z. Khan, M. H. Memon, S. Ur Rahman, M. Sajjad, F. Lin and L. Sun, "A Single-Fed Multiband Antenna for WLAN and 5G Applications", *Sensors. Lett.*, vol. 20, pp. 1-13, November 2020.
- [15] S. Alani, Z. Zakaria, T. Saeidi, A. Ahmad, H. Alsariera, O. S. Al-Heety, and S. N. Mahmood, "Electronic bandgap miniaturized UWB antenna for near-field microwave investigation of skin", *AIP Advances*, vol. 11, article. 035228, 2021
- [16] I. Slomian, K. Wincza and S. Gruszczynski, "Low-Cost Broadband Microstrip Antenna Array for 24 GHz FMCW Radar Applications", *International Journal of RF and Microwave Computer-Aided Engineering*, vol. 23, no. 4, pp. 499-506, July 2013.
- [17] P. Squadrito, S. Zhang and G. F. Pedersen, "X-Band Dual Circularly Polarized Patch Antenna with High Gain for Small Satellites", *IEEE Access*, vol. 7, pp. 74925-74930, May 2019.
- [18] T. Su, X. Yi, and B. Wu, "X/Ku Dual-Band Single-Layer Reflectarray Antenna", *IEEE Antennas and Wireless Propagation Letters*, vol. 18, no. 2, pp. 338-342, February 2019.
- [19] J-S. Park, J-B. Ko, H-K. Kwon, B-S. Kang, B. Park and D. Kim, "A Tilted Combined Beam Antenna for 5G Communications Using a 28-GHz Band", *IEEE Antennas and Wireless Propagation Letters*, vol. 15, pp 1685-1688, 2016.
- [20] R. Mondal, P. S. Reddy, D. C. Sarkar and P. P. Sarkar, "Compact ultra-wideband antenna: improvement of gain and FBR across the entire bandwidth using FSS", *IET Microwaves, Antennas & Propagation*, vol. 14, pp. 66-74, 2020.
- [21] M. K. Pain, S. Bhunia, S. Biswas, D. Sarkar and P. P. Sarkar, "A novel investigation on size reduction of a frequency selective surface", *Microwave and Optical Technology Letters*, vol. 49, no. 11, pp. 2820-2821, November 2007.
- [22] S. Maity, T. Tewary, S. Mukherjee, A. Roy, Dr. P. P. Sarkar and Dr. S. Bhunia, "Super Wideband High Gain Hybrid Microstrip Patch Antenna", *International Journal of Electronics and Communications(AEU)*, May 2022.
- [23] T. Tewary, S. Maity, S. Mukherjee, A. Roy, Dr. P. P. Sarkar and Dr. S. Bhunia, "Design of high gain broadband microstrip patch antenna for UWB/X/Ku band applications", *International Journal of Electronics and Communications*, vol. 139, September 2021.
- [24] T. Tewary, S. Maity, S. Mukherjee, A. Roy, Dr. P. P. Sarkar and Dr. S. Bhunia, "High gain miniaturized super-wideband microstrip patch antenna", *International Journal of Communication Systems*, April 28 2022.
- [25] S. Maity, T. Tewary, S. Mukherjee, A. Roy, Dr. P. P. Sarkar and Dr. S. Bhunia, "Wideband hybrid microstrip patch antenna and gain improvement using frequency selective surface", *International Journal of Communication Systems*, June 2022.
- [26] C. A. Balanis, *Antenna Theory, Analysis and Design*. 4th Edition, Wiley, ISBN 978-1-118-642060-1.
- [27] B. A. Munk, *Frequency selective surfaces: theory and design*. Wiley, New York, 2000